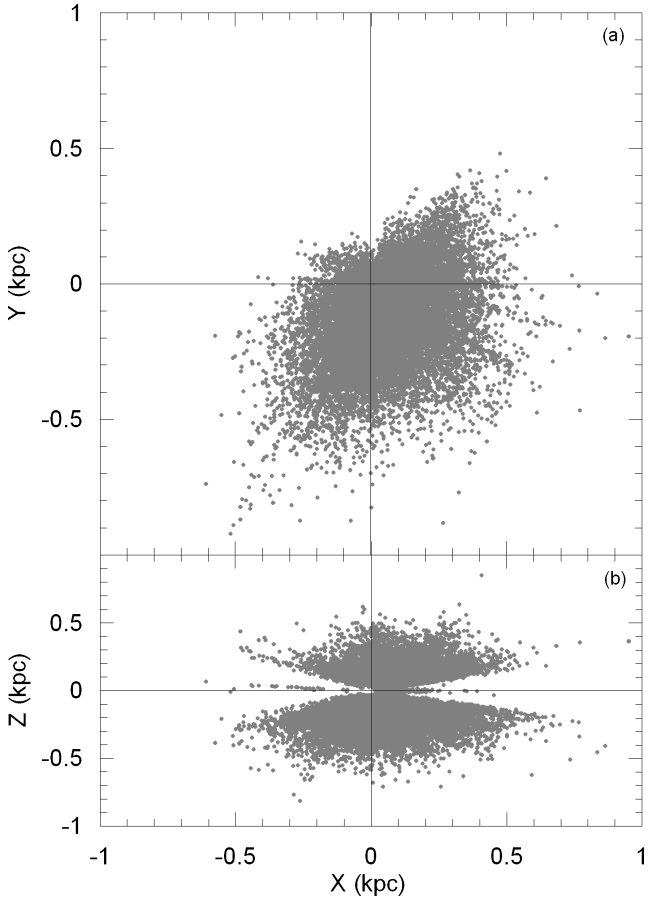

Figure 4. Space distributions of RAVE main-sequence stars on two planes: (a) *X*–*Y* and (b) *X*–*Z*.

In the calculations, the epoch of J2000 was adopted as described in the International Celestial Reference System of the *Hipparcos* and *Tycho-2* Catalogues (ESA 1997). The transformation matrices use the notation of a right-handed system. Hence, U, V and W are the components of a velocity vector of a star with respect to the Sun, where U is positive towards the Galactic Centre ($l = 0^\circ, b = 0^\circ$), V is positive in the direction of Galactic rotation ($l = 90^\circ, b = 0^\circ$) and W is positive towards the North Galactic Pole ($b = 90^\circ$).

Correction for differential Galactic rotation is necessary for accurate determination of U, V and W velocity components. The effect is proportional to the projection of the distance to the stars on to the Galactic plane, i.e. the W velocity component is not affected by Galactic differential rotation (Mihalas & Binney 1981). We applied the procedure of Mihalas & Binney (1981) to the distribution of the sample stars in the *X*–*Y* plane and estimated the first order Galactic differential rotation corrections for U and V velocity components of the sample stars. The range of these corrections is $-25.13 < \mathrm{d}U < 13.07$ and $-1.46 < \mathrm{d}V < 2.28\,\mathrm{km\,s^{-1}}$ for U and V, respectively. As expected, U is affected more than the V component. Also, the high values for the U component show that corrections for differential Galactic rotation cannot be ignored.

The uncertainties of the space velocity components $U_{\rm err}$, $V_{\rm err}$ and $W_{\rm err}$ were computed by propagating the uncertainties of the proper motions, distances and radial velocities, again using a (standard) algorithm by Johnson & Soderblom (1987). Then, the error for the total space motion of a star follows from the equation:

$$S_{\rm err}^2 = U_{\rm err}^2 + V_{\rm err}^2 + W_{\rm err}^2. \quad (4)$$

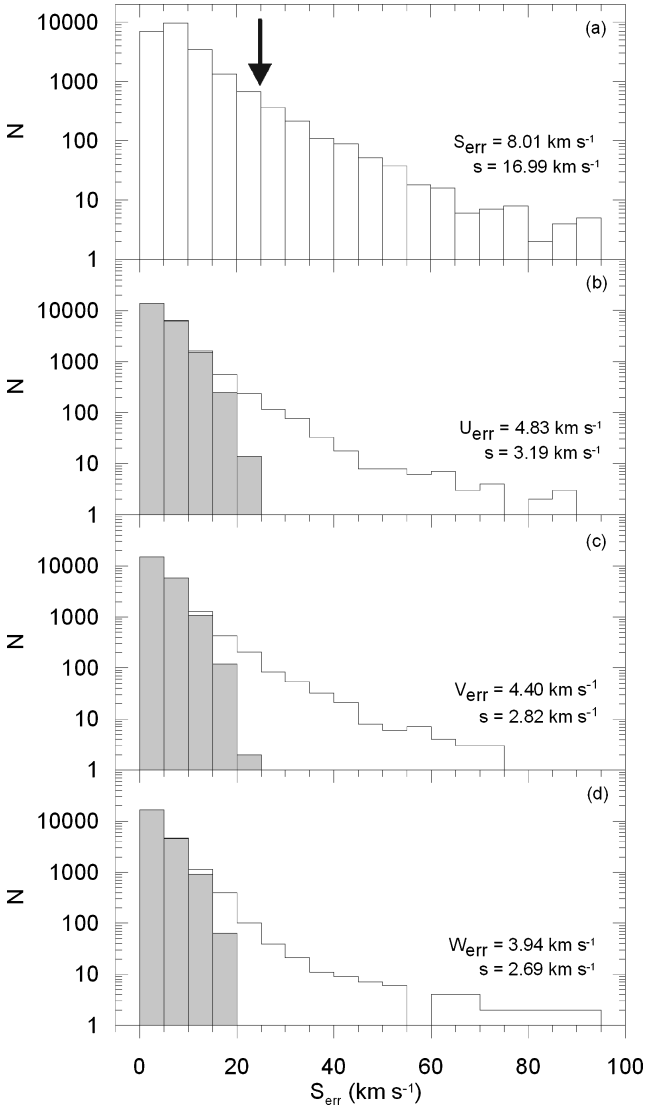

Figure 5. Error histograms for space velocity (panel a) and its components (panels b–d) for RAVE main-sequence stars. The arrow in panel (a) indicates the upper limit of the total error adopted in this work. The shaded part of the histogram indicates the error for different velocity components of stars after removing the stars with large space velocity errors.

The distributions of errors for both the total space motion and that in each component are plotted in Fig. 5. The median and standard deviation for space velocity errors are $\tilde{S}_{\rm err} = 8.01\,\mathrm{km\,s^{-1}}$ and $s = 16.99\,\mathrm{km\,s^{-1}}$, respectively. We now remove the most discrepant data from the analysis, knowing that outliers in a survey such as this will preferentially include stars which are systematically misanalysed binaries, etc. Thus, we omit stars with errors that deviate by more than the sum of the standard error and the standard deviation, i.e. $S_{\rm err} > 25\,\mathrm{km\,s^{-1}}$. This removes 867 stars, 4 per cent of the sample. Thus, our sample was reduced to 20 453 stars, those with more robust space velocity components. After applying this constraint, the median values and the standard deviations for the velocity components were reduced to $(\tilde{U}_{\rm err}, \tilde{V}_{\rm err}, \tilde{W}_{\rm err}) = (4.83 \pm 3.19, 4.40 \pm 2.82, 3.94 \pm 2.69)\,\mathrm{km\,s^{-1}}$. The two-dimensional distribution of the velocity components for the reduced sample is given in Fig. 6. The most interesting feature for our present analysis in the (U, V) and (V, W) diagrams is the offsets of the zero-points of the sample stars from the origins

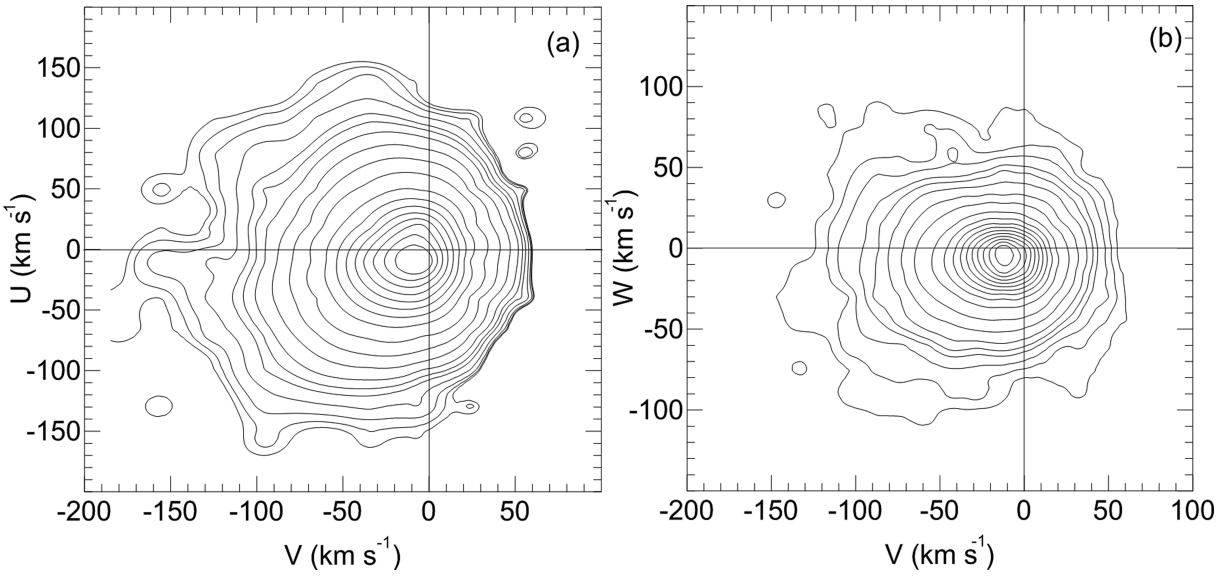

Figure 6. The distribution of velocity components of RAVE main-sequence stars in two projections on to the Galactic plane: (a) U–V and (b) W–V.

of the coordinate systems – these correspond to the solar velocity components.

5 POPULATION ANALYSIS

We now wish to consider the population kinematics as a function of stellar population, using space motion as a statistical process to label stars as (probabilistic) 'members' of a stellar population. We used the procedure of Bensby, Feltzing & Lundström (2003) and Bensby et al. (2005) to allocate the main-sequence sample (20 453 stars) into populations and derived the solar space velocity components for the thin-disc population to check the dependence of LSR parameters on population. Bensby et al. (2003, 2005) assumed that the Galactic space velocities of stellar populations with respect to the LSR have Gaussian distributions as follows:

$$f(U,\ V,\ W) = k \exp\left(-\frac{U_{\rm LSR}^2}{2\sigma_{U_{\rm LSR}}^2} - \frac{(V_{\rm LSR} - V_{\rm asym})^2}{2\sigma_{V_{\rm LSR}}^2} - \frac{W_{\rm LSR}^2}{2\sigma_{W_{\rm LSR}}^2}\right), \quad (5)$$

where

$$k = \frac{1}{(2\pi)^{3/2}\sigma_{U_{\rm LSR}}\sigma_{V_{\rm LSR}}\sigma_{W_{\rm LSR}}} \quad (6)$$

normalizes the expression. For consistency with other analyses, we adopt $\sigma_{U_{\rm LSR}}$, $\sigma_{V_{\rm LSR}}$ and $\sigma_{W_{\rm LSR}}$ as the characteristic velocity dispersions: 35, 20 and 16 km s^{-1} for thin disc (D); 67, 38 and 35 km s^{-1} for thick disc (TD); 160, 90 and 90 km s^{-1} for halo (H), respectively (Bensby et al. 2003). $V_{\rm asym}$ is the asymmetric drift: -15, -46 and -220 km s^{-1} for thin disc, thick disc and halo, respectively. $U_{\rm LSR}$, $V_{\rm LSR}$ and $W_{\rm LSR}$ are LSR velocities. The space velocity components of the sample stars relative to the LSR were estimated by adding the values for the space velocity components evaluated by Dehnen & Binney (1998) to the corresponding solar ones.

The probability of a star of being 'a member' of a given population is defined as the ratio of the $f(U, V, W)$ distribution functions times the ratio of the local space densities for two populations. Thus,

$$\mathrm{TD/D} = \frac{X_{\rm TD}}{X_{\rm D}} \times \frac{f_{\rm TD}}{f_{\rm D}} \qquad \mathrm{TD/H} = \frac{X_{\rm TD}}{X_{\rm H}} \times \frac{f_{\rm TD}}{f_{\rm H}} \quad (7)$$

Table 2. The space velocity component ranges for population types of RAVE main-sequence stars.

Parameters	U (km s^{-1})	V (km s^{-1})	W (km s^{-1})
TD/D ≤ 0.1	$(-85, 75)$	$(-80, 40)$	$(-55, 40)$
$0.1 <$ TD/D ≤ 1	$(-105, 100)$	$(-100, 50)$	$(-70, 50)$
TD/D > 1	$(-165, 155)$	$(-175, 60)$	$(-115, 90)$

are the probabilities for a star of it being classified as a thick-disc star relative to being a thin-disc star, and relative to being a halo star, respectively. $X_{\rm D}$, $X_{\rm TD}$ and $X_{\rm H}$ are the local space densities for thin disc, thick disc and halo, i.e. 0.94, 0.06 and 0.0015, respectively (Robin et al. 1996; Buser, Rong & Karaali 1999). We followed the argument of Bensby et al. (2005) and separated the sample stars into four categories: TD/D ≤ 0.1 (high-probability thin-disc stars), $0.1 <$ TD/D ≤ 1 (low-probability thin-disc stars), $1 <$ TD/D ≤ 10 (low-probability thick-disc stars) and TD/D > 10 (high-probability thick-disc stars). It turned out that 18 026 and 1552 stars of the sample were classified as high and low-probability thin-disc stars, respectively, whereas 412 and 463 stars are probabilistically thick disc and halo. The ranges and distributions of the Galactic space velocity components for our different stellar population categories are given in Table 2 and Fig. 7.

6 RESULTS

We analysed the U, V and W space velocity components for the main-sequence sample (20 453 stars) as well as for four subsamples, i.e. high-probability thin-disc stars of different spectral types (i) F, G and K($N = 17889$ stars), (ii) F($N = 9654$ stars), (iii) G($N = 5910$ stars), (iv) K($N = 2325$ stars) and estimated the modes of the Gaussian distributions for each category and each space velocity component. Spectral types were determined according to the 2MASS colours of the stars (Bilir et al. 2008, see Table 3). The colour range is $0.08 < J - H \leq 0.30$ for F spectral type and $0.30 < J - H \leq 0.42$ for G spectral type. The modes of these kinematic distribution functions are the best estimators of the (negative) value of the solar motion relative to the LSR values for the stellar group

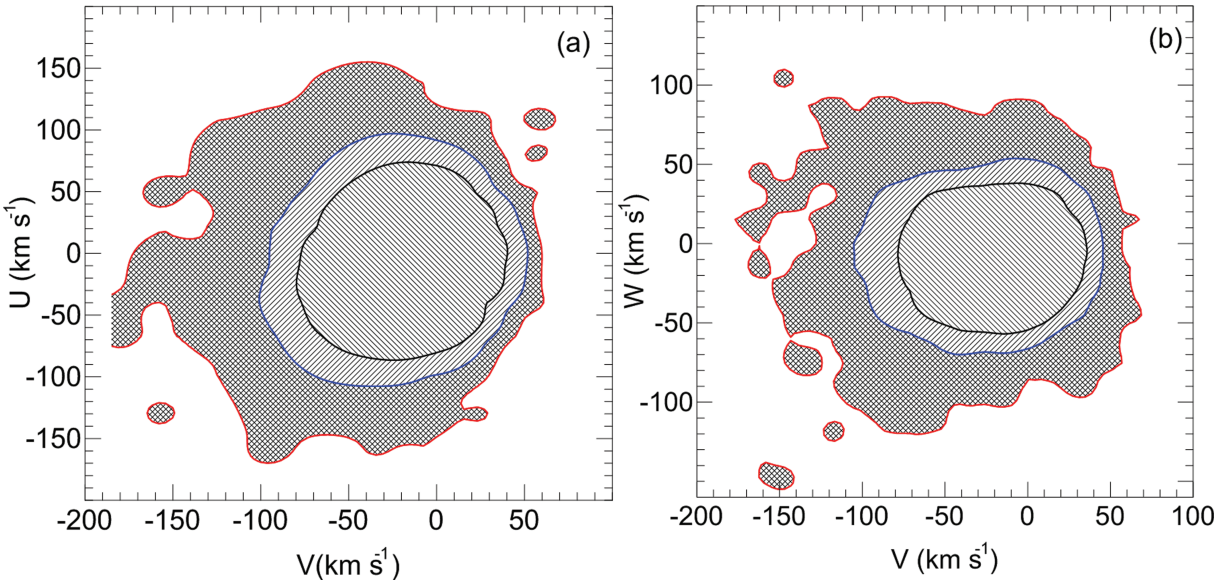

Figure 7. Distribution of main-sequence stars of different population types on two Galactic space velocity planes: (a) U–V and (b) W–V. The contours indicate (outwards from the centre) high-probability thin disc (TD/D ≤ 0.1), low-probability thin disc ($0.1 <$ TD/D ≤ 1) and low- and high-probability thick disc and halo stars (TD/D > 1).

Table 3. Space velocity components of the Sun with respect to the LSR for five population subsamples, as described in the text.

Parameters	Colour range	U (km s^{-1})	V (km s^{-1})	W (km s^{-1})	N
All sample	$0.05 \leq (J-H)_0 \leq 0.55$	8.83 ± 0.24	14.19 ± 0.34	6.57 ± 0.21	20 453
TD/D ≤ 0.1	$0.05 \leq (J-H)_0 \leq 0.55$	8.50 ± 0.29	13.38 ± 0.43	6.49 ± 0.26	18 026
F spectral type	$0.08 < (J-H)_0 \leq 0.30$	8.35 ± 0.36	13.14 ± 0.43	6.24 ± 0.27	9 654
G spectral type	$0.30 < (J-H)_0 \leq 0.42$	9.25 ± 0.50	14.42 ± 0.57	6.67 ± 0.38	5 910
K spectral type	$0.42 < (J-H)_0 \leq 0.55$	7.01 ± 0.67	11.96 ± 0.66	7.03 ± 0.38	2 325

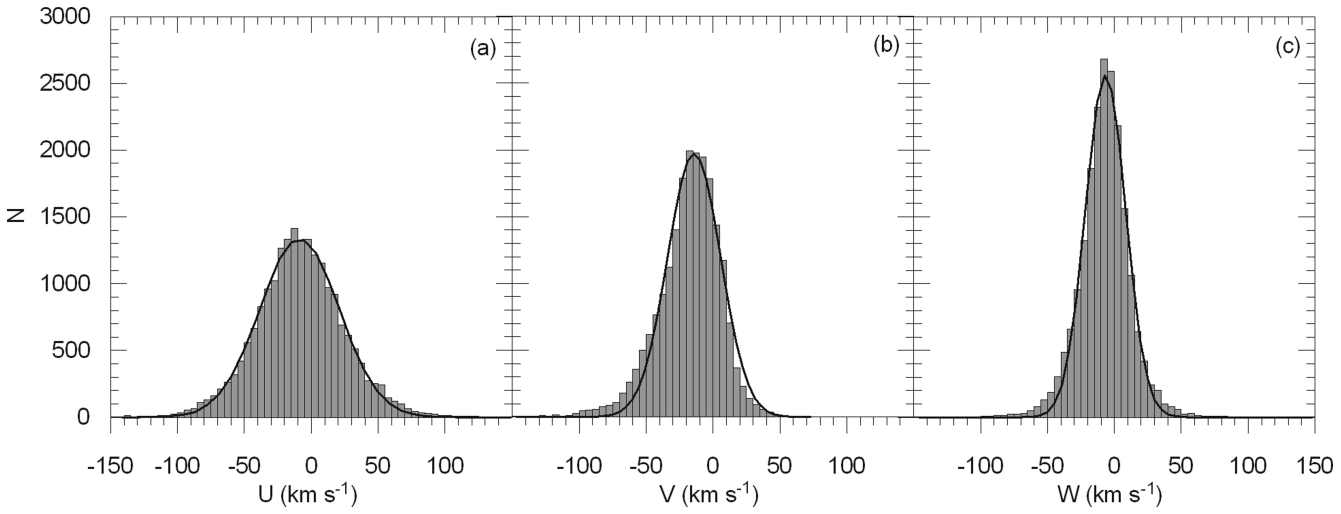

Figure 8. The distribution functions of Galactic space velocities for the 20 453 main-sequence stars, with overlaid best-fitting Gaussian distributions.

in question. The histograms for the space velocity components for the main-sequence star sample are given in Fig. 8. Gaussian fits, which are clearly an adequate description of the data, reveal $U_\odot = 8.83 \pm 0.24$, $V_\odot = 14.19 \pm 0.34$ and $W_\odot = 6.57 \pm 0.21$ km s^{-1} as the modes of the corresponding histograms. The modes of the histograms for the space velocity components for high-probability thin-disc stars of F, G and K spectral types, obtained by fitting them to the Gaussian distributions (Fig. 9), are a little different than the preceding set, i.e. $U_\odot = 8.50 \pm 0.29$, $V_\odot = 13.38 \pm 0.43$ and $W_\odot = 6.49 \pm 0.26$ km s^{-1}. The largest difference in $V_\odot$ can be confirmed by comparing Figs 8(b) and 9(b) (see Section 7 below for details).

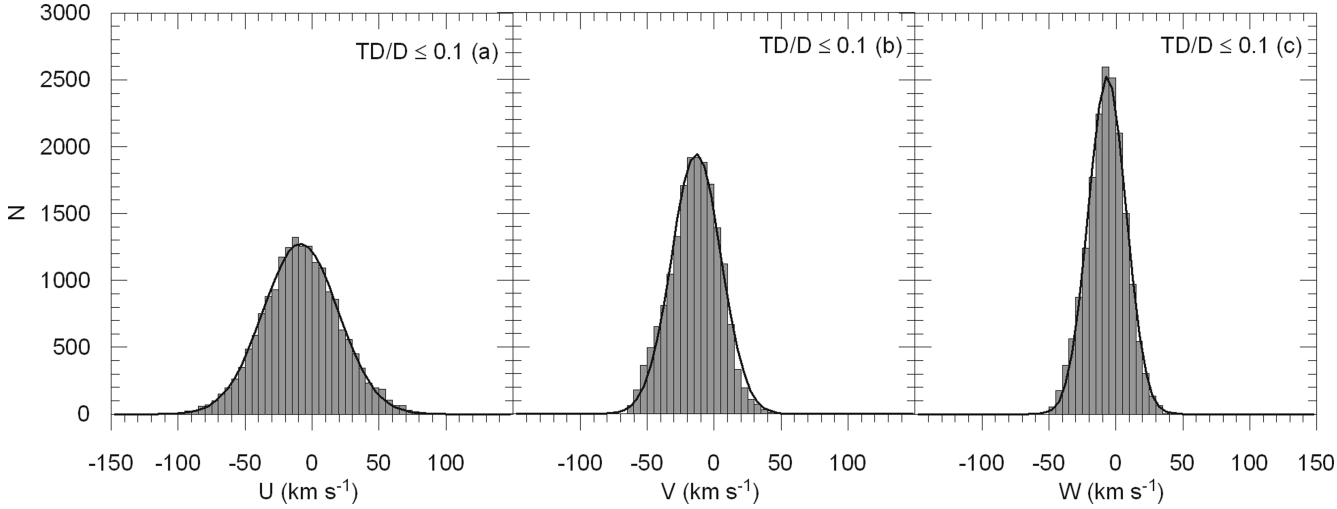

Figure 9. The distribution functions of Galactic space velocities for the high-probability thin-disc stars, with overlaid best-fitting Gaussian distributions.

The distribution functions of Galactic space velocity components for high-probability thin-disc stars, using our kinematic population assignment process, and presented separately for each of three spectral-type groups, are given in Table 3. We evaluated the modes for each distribution from the best-fitting Gaussian. These results are also given in Table 3, together with those for the high-probability main-sequence star sample and for the full sample. There are differences between the modes of the corresponding space velocity components for stars with *F*, *G* and *K* spectral types as well as between these modes and the corresponding ones for other subsamples which will be discussed in Section 7.

7 DISCUSSION

By definition, the LSR is the reference frame of a hypothetical star at the Galactocentric distance of the Sun, and in the Galactic plane, that would be on a circular orbit in the gravitational potential of the Galaxy. We can attribute *U*, *V* and *W* velocity components of the Sun relative to this hypothetical star by observing the kinematic distribution function of stars at the solar neighbourhood, provided the stellar comparison sample we use is in dynamical equilibrium. We can similarly test the equilibrium state of stellar populations by comparing their deduced solar peculiar motion, or equivalently their mean motion relative to an LSR. One may wonder if the kinematically cold thin-disc stars feel a large asymmetric gravitational potential from, perhaps, an inner Galactic bar. Do spiral arms have systematic kinematic effects visible in young stars? Is the LSR defined by the high-velocity halo stars, which feel largely extended dark matter potentials, the same as that of thick-disc stars and thin-disc stars? These questions essentially repeat a query on the closeness of the higher order Oort constants to zero, for all Galactic components.

The significance is such one wishes to determine the 'solar peculiar velocity' for many samples, using several techniques. Doing this (see Table 1 above for a list) has led, in general, to determinations of the peculiar motion radially outwards from the Galactic Centre $U_\odot$ which are consistent and small, independent of the comparison sample chosen. Every stellar sub-population in the Galaxy seems remarkably radially stable and circularly symmetric, with no evidence for bar-like perturbations. Similarly, doing this for the net vertical motion $W_\odot$ provides the same conclusion. The sky fails to fall (see also Seabroke & Gilmore 2008). The Galaxy, locally, seems not be significantly affected by an accreted stellar system, or asymmetric mass infall. The situation is less clear in the rotational direction, $V_\odot$. Here, there is less agreement between determinations, largely since model-dependent assumptions need to be made to correct kinematics for energy balance, which transfers angular momentum systematically into random motions with time. This may happen by slow diffusion, or by more dramatic radially dependent effects. The relevant way forward is to determine $V_\odot$ as a function of as many definable 'populations' as is feasible, in many ways. We follow that approach here, where we find, in agreement with several recent studies, a value of $V_\odot$ near 13 km s^{-1}. We determine this value with respect to three subgroups of local main-sequence stars. These groups cover a very wide range of stellar ages. Yet they agree, statistically, with each other, and with other determinations based on more local samples. The concept of an LSR again seems well defined.

We study stars which are thin-disc dwarfs like the Sun. We expect a dispersion in the distribution of the velocity components due to their inherent distributions and differences between the same velocity components of sample stars of different population types and ages. The way to reveal the corresponding velocity component is to fit the space motion data to a suitable distribution function. Encouragingly, a simple Gaussian provides an excellent approximation so we can identify the mean solar motion with its mode. This is the procedure we used in this work.

The star sample was taken from RAVE, which extends much beyond the distance of the high-precision local *Hipparcos* sample, i.e. 97 per cent of the sample lies within the distance interval $0 < d \leq 0.6$ kpc. We applied the following constraints to obtain a main-sequence sample with relatively small errors: (i) we selected stars with surface gravity $4 < \log g < 5$; (ii) we omitted stars with $(J - H)_0 < 0.05$ and $(J - H)_0 > 0.55$ to avoid blue horizontal branch and red giant stars; (iii) we excluded stars with space velocity errors larger than 25 km s^{-1} and (iv) we separated stars probabilistically according to their population types, and we used the high-probability thin-disc sample to minimize contamination by thick-disc/halo stars as a preferred sample in our work. We estimated solar space velocity components for five samples for all our RAVE main-sequence stars, for the subsample of high-probability thin-disc main-sequence stars and separately for the thin-disc main-sequence stars of *F*, *G* and *K*

spectral types. The results (see Table 3 above) are consistent, within sampling errors, across all subsamples. They are also in agreement with recent determinations using other population subsamples, and over very different ranges. There is increasing agreement that the solar peculiar velocity in the rotation direction has been underestimated in older studies. The internal agreement between our different samples, and between this study and others, provides evidence that the Galactic potential near the Sun is symmetric, with no evident time-dependent variation.

ACKNOWLEDGMENTS

We thank the anonymous referee for his/her comments. Funding for RAVE has been provided by the Australian Astronomical Observatory, the Astrophysical Institute Potsdam, the Australian National University, the Australian Research Council, the French National Research Agency, the German Research Foundation, the Istituto Nazionale di Astrofisica at Padova, The Johns Hopkins University, the W.M. Keck Foundation, the Macquarie University, the Netherlands Research School for Astronomy, the Natural Sciences and Engineering Research Council of Canada, the Slovenian Research Agency, the Swiss National Science Foundation, the Science & Technology Facilities Council of the UK, Opticon, Strasbourg Observatory, and the Universities of Groningen, Heidelberg and Sydney.

This work has been supported in part by the Scientific and Technological Research Council (TÜBİTAK) 108T613. SK is grateful to the Beykent University for financial support. This publication makes use of data products from the Two Micron All Sky Survey, which is a joint project of the University of Massachusetts and the Infrared Processing and Analysis Center/California Institute of Technology, funded by the National Aeronautics and Space Administration and the National Science Foundation.

This research has made use of the SIMBAD, NASA's Astrophysics Data System Bibliographic Services and the NASA/IPAC ExtraGalactic Data base (NED) which is operated by the Jet Propulsion Laboratory, California Institute of Technology, under contract with the National Aeronautics and Space Administration.

REFERENCES

Bahcall J. N., Soneira R. M., 1980, ApJS, 44, 73
Bensby T., Feltzing S., Lundström I., 2003, A&A 410, 527
Bensby T., Feltzing S., Lundström I., Ilyin I., 2005, A&A, 433, 185
Bilir S., Karaali S., Ak S., Yaz E., Cabrera-Lavers A., Coşkunoğlu K. B., 2008, MNRAS, 390, 1569
Binney J. J., 2010, MNRAS, 401, 2318
Binney J. J., Dehnen W., Houk N., Murray C. A., Penston M. J., 1997, ESA-SP 402, Proc. ESA Symp. *Hipparcos*, p. 473
Bobylev V. V., Bajkova A. T., 2007, Astron. Rep., 51, 372
Bobylev V. V., Bajkova A. T., 2010, MNRAS, 408, 1788
Breddels M. A. et al., 2010, A&A, 511, 90
Buser R., Rong J., Karaali S., 1999, A&A, 348, 98
Dehnen W., Binney J. J., 1998, MNRAS, 298, 387
ESA, 1997, The *Hipparcos* and *Tycho* Catalogues, ESA SP-1200. ESA, Noordwijk
Fiorucci M., Munari U., 2003, A&A, 401, 781
Francis C., Anderson E., 2009, New Astron., 14, 615
Gilmore G., Wyse R. F. G., Kuijken K., 1989, ARA&A, 27, 555
Homann H., 1886, Astron. Nachr., 114, 25
Johnson D. R. H., Soderblom D. R., 1987, AJ, 93, 864
Katz D. et al., 2004, MNRAS, 354, 1223
McMillan P., Binney J., 2010, MNRAS, 402, 934
Marshall D. J., Robin A. C., Reylé C., Schultheis M., Picaud S., 2006, A&A, 453, 635
Mignard F., 2000, A&A, 354, 522
Mihalas D., Binney J., 1981, Galactic Astronomy: Structure and Kinematics, 2nd edn. W.H. Freeman and Co., San Francisco
Munari U., 2003, in ASP Conf. Ser. Vol. 298, GAIA Spectroscopy: Science and Technology. Astron. Soc. Pac., San Francisco, p. 51
Pasetto S., Grebel E. K., the RAVE Collaboration, 2010, BAAS, 42, 478
Piskunov A. E., Kharchenko N. V., Röser S., Schilbach E., Scholz R.-D., 2006, A&A, 445, 545
Reid M. J. et al., 2009, ApJ, 700, 137
Robin A. C., Haywood M., Créze M., Ojha D. K., Bienaymé O., 1996, A&A, 305, 125
Rygl K. L. J., Brunthaler A., Reid M. J., Menten K. M., van Langevelde H. J., Xu Y., 2010, A&A, 511, 2
Schlegel D. J., Finkbeiner D. P., Davis M., 1998, ApJ, 500, 525
Schönrich R., Binney J., Dehnen W., 2010, MNRAS, 403, 1829
Seabroke G. M., Gilmore G., the RAVE Collaboration, 2008, MNRAS, 384, 11
Steinmetz M. et al., 2006, AJ, 132, 1645
Strömberg G., 1946, ApJ, 104, 12
Veltz L. et al., 2008, A&A, 480, 753
Wilkinson M. I. et al., 2005, MNRAS, 359, 1306
Zwitter T. et al., 2008, AJ, 136, 421

This paper has been typeset from a TEX/LATEX file prepared by the author.